2692 *Inorg. Chem.* **2010**, *49*, 2692–2700
DOI: 10.1021/ic901920y

Inorganic Chemistry
Article

Sn(IV) Porphyrin Based Axial-Bonding Type Porphyrin Triads Containing Heteroporphyrins as Axial Ligands

Vijayendra S. Shetti and Mangalampalli Ravikanth*

Department of Chemistry, Indian Institute of Technology, Bombay, Powai, Mumbai 400 076, India

Received September 29, 2009

The thiaporphyrin building blocks with N_3S and N_2S_2 cores containing one hydroxyphenyl functional group at the *meso* position were synthesized by adopting the unsymmetrical thiophene diol method. These monohydroxy thiaporphyrins were used to construct the first examples of axial bonding type Sn(IV) porphyrin triads in which Sn(IV) porphyrin acts as basal unit and the two thiaporphyrin units as axial ligands by treating with $SnTTP(OH)_2$ in benzene at refluxing temperature. The axial bonding type triads were confirmed by mass, 1D and 2D NMR studies. The absorption and electrochemical studies support weak ground state interaction among the porphyrin subunits within the porphyrin triads. The fluorescence studies indicate there is a possibility of energy transfer at the singlet state from basal Sn(IV) porphyrin unit to axial thiaporphyrin units.

Introduction

Multiporphyrin arrays have attracted attention because of their use in opto-electronic device applications and light harvesting.[1] Porphyrins and metalloporphyrins can be assembled into arrays either by covalent strategies[1] or by adopting non-covalent strategies.[2] Conventional linear synthetic strategies are quite limiting since these strategies normally involve many sequential steps, separation of statistical mixtures, and extensive chromatographic purification, always resulting in a low product yield. Non-covalent strategies have emerged as a viable alternative to covalent synthesis in the construction of multiporphyrin arrays. Both coordination and multiple hydrogen bonds or their combination have been used as the source of the non-covalent bonding interactions.[2] To construct non-covalent porphyrin arrays, the porphyrins and metalloporphyrins were exploited essentially in two ways: (1) Metalloporphyrins can be acceptor building blocks provided that the metal atom inside the porphyrin core has at least one axial site available for coordination. (2) Porphyrins can behave as donor building blocks, provided that they have ligands appended to the periphery that can suitably coordinate to metal centers. These two kinds of porphyrin modules, acceptor and donor, can be freely and rationally combined to build multiporphyrin self-assembling systems. When porphyrins bearing external coordination functionalities bind to other metalloporphyrins, assemblies of axially connected chromophores commonly known as "axial bonding type" arrays are generated.[3] Tailor-made metalloporphyrins bearing nitrogen and oxygen donor functionalities have been designed that spontaneously self-assemble in discrete arrays by virtue of the independent coordination properties of Zn(II), Ru(II), Rh(III), and Sn(IV) centers.

Tin(IV) porphyrins offer the chemist many advantages because of the particular properties conferred by the highly charged main group metal center.[4] The Sn(IV) porphyrins are very stable, diamagnetic, and usually six coordinate with trans-diaxial anionic or occasionally neutral ligands. The particular oxophilicity of the Sn(IV) center confers a notable preference for coordination of carboxylates and aryloxides, and these properties have been exploited by different workers for the preparation of elegant and elaborate multiporphyrin arrays.[4] The oxophilic nature of Sn(IV) ions has been used by Maiya and co-workers[5] to construct novel axial-bonding type porphyrin arrays such as porphyrin trimers, hexamers,

*To whom correspondence should be addressed. E-mail: ravikanth@chem.iitb.ac.in.

(1) (a) Suslick, K. S.; Rakow, N. A.; Kosal, M. E.; Chou, J.-H. *J. Porphyrins Phthalocyanines* **2000**, *4*, 407–413. (b) Burrell, A. K.; Officer, D. L.; Plieger, P. G.; Reid, D. C. W. *Chem. Rev.* **2001**, *101*, 2751–2796. (c) Shinokubo, H.; Osuka, A. *Chem. Commun.* **2009**, 1011–1021.

(2) (a) Imamura, T.; Fukushima, K. *Coord. Chem. Rev.* **2000**, *198*, 133–156. (b) Wojaczynski, J.; Latos-Grazynski, L. *Coord. Chem. Rev.* **2000**, *204*, 113–171.

(3) (a) Aoyama, Y.; Kamohara, T.; Yamagishi, A.; Toi, H.; Ogoshi, H. *Tetrahedron Lett.* **1987**, *28*, 2143–2146. (b) Stibrany, R. T.; Vasudevan, J.; Knapp, S.; Potenza, J. A.; Emge, T.; Schugar, H. J. *J. Am. Chem. Soc.* **1996**, *118*, 3980–3981. (c) Gerasimchuk, N. N.; Mokhir, A. A.; Rodgers, K. R. *Inorg. Chem.* **1998**, *37*, 5641–5650. (d) Funatsu, K.; Imamura, T.; Ichimura, A.; Sasaki, Y. *Inorg. Chem.* **1998**, *37*, 4986–4995. (e) Vasudevan, J.; Stibrany, R. T.; Bumby, J.; Knapp, S.; Potenza, J. A.; Emge, T. J.; Schugar, H. J. *J. Am. Chem. Soc.* **1996**, *118*, 11676–11677. (f) Kariya, N.; Imamura, T.; Sasaki, Y. *Inorg. Chem.* **1998**, *37*, 1658–1668.

(4) Arnold, D. P.; Blok, J. *Coord. Chem. Rev.* **2004**, *248*, 299–319.

(5) (a) Giribabu, L.; Rao, T. A.; Maiya, B. G. *Inorg. Chem.* **1999**, *38*, 4971–4980. (b) Kumar, A. A.; Giribabu, L.; Reddy, D. R.; Maiya, B. G. *Inorg. Chem.* **2001**, *40*, 6757–6766.

 Published on Web 02/19/2010

Scheme 1. Synthesis of Monohydroxy Porphyrin Building Blocks **3** and **4**

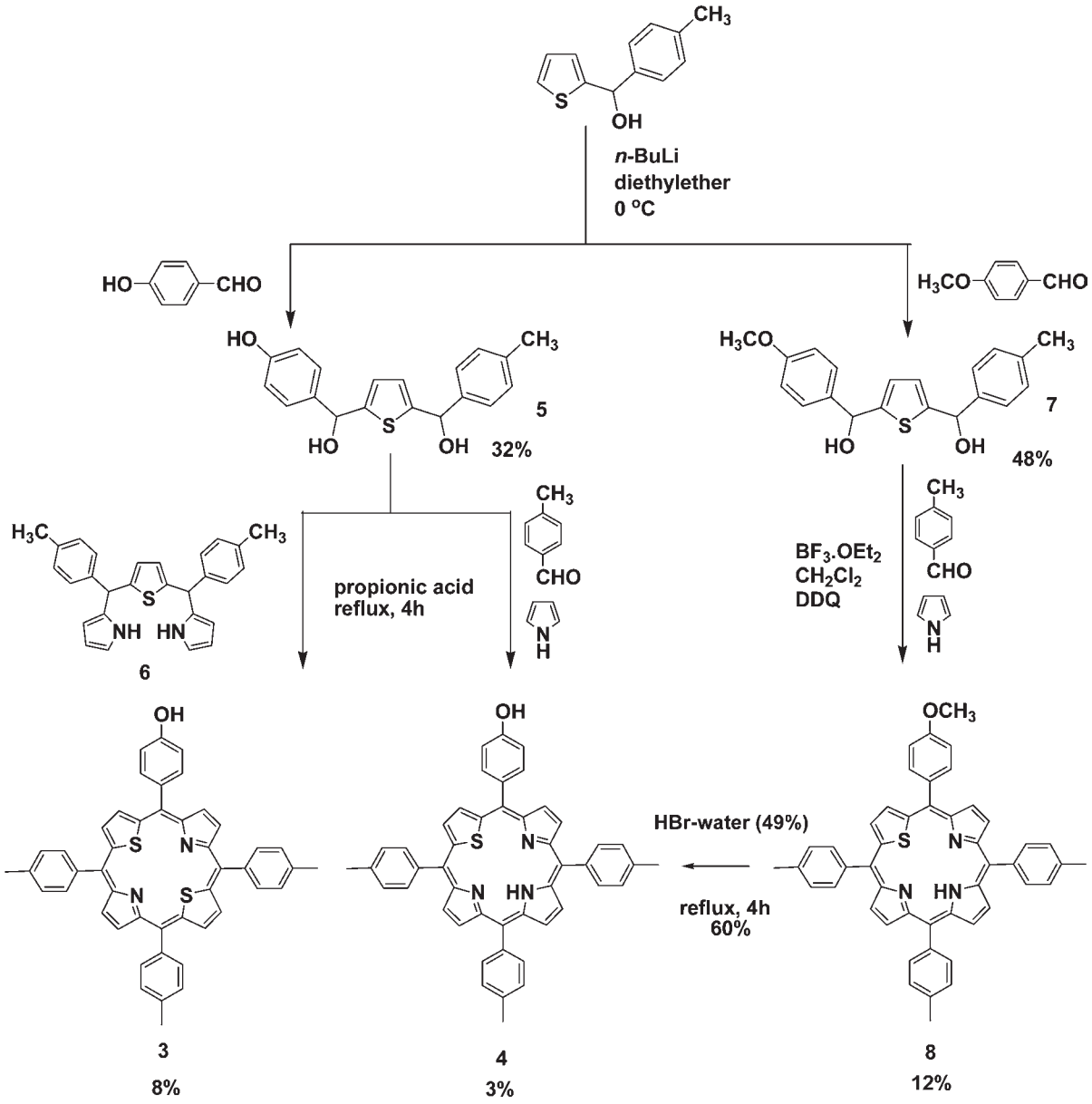

and nonamers, and they have studied their electrochemical and photophysical properties in detail. Sanders and co-workers[6] and others[7] have also used the oxophilic nature of Sn(IV) centers along with complementary binding properties of Ru(II) or Zn(II) toward nitrogen and synthesized several supramolecular porphyrin arrays. A common feature among the axial bonding type Sn(IV) porphyrin arrays reported in literature[4−7] so far is that all porphyrin subunits in these arrays have similar donor atoms (pyrrole nitrogens) in the porphyrin core. One area of porphyrin chemistry that has received less attention but may lead to systems of interesting structural and electronic properties is the characterization of porphyrin arrays containing two dissimilar macrocycles such as porphyrin-chlorin,[8a] porphyrin corrole,[8b] porphyrin-phthalocyanine[8c] and porphyrin-heteroporphyrin.[8d] We[9a−d] and others[9e,f] reported synthesis of covalent and non-covalent porphyrin arrays containing two dissimilar cores such as

(6) (a) Hawley, J. C.; Bampos, N. B.; Abraham, R. J.; Sanders, J. K. M. *Chem. Commun.* **1998**, 661–662. (b) Kim, H.-J.; Bampos, N.; Sanders, J. K. M. *J. Am. Chem. Soc.* **1999**, *121*, 8120–8121. (c) Maiya, B. G.; Bampos, N.; Kumar, A. A.; Feeder, N.; Sanders, J. K. M. *New J. Chem.* **2001**, *25*, 797–800. (d) Webb, S. J.; Sanders, J. K. M. *Inorg. Chem.* **2000**, *39*, 5920–5929.

(7) (a) Fallon, G. D.; Lee, M. A.-P.; Langford, S. J.; Nichols, P. J. *Org. Lett.* **2002**, *4*, 1895–1898. (b) Langford, S. J.; Latter, M. J.; Beckmann, J. *Inorg. Chem. Commun.* **2005**, *8*, 920–923. (c) Langford, S. J.; Woodward, C. P. *CrystEngComm* **2007**, *9*, 218–221. (d) Kim, H.-J.; Jo, H. J.; Kim, J.; Kim, S.-Y.; Kim, D.; Kim, K. *CrystEngComm* **2005**, *7*, 417–420. (e) Jo, H. J.; Jung, S. H.; Kim, H.-J. *Bull. Korean Chem. Soc.* **2004**, *25*, 1869–1873.

(8) (a) Paolesse, R.; Pandey, R. K.; Forsyth, T. P.; Jaquinod, L.; Gerzevske, K. R.; Nurco, D. J.; Senge, M. O.; Licoccia, S.; Boschi, T.; Smith, K. M. *J. Am. Chem. Soc.* **1996**, *118*, 3869–3882. (b) Flamingi, L.; Ventura, B.; Tasior, M.; Gryko, D. T. *Inorg. Chim. Acta* **2007**, *360*, 803–813. (c) Yang, S. I.; Li, J.; Cho, H. S.; Kim, D.; Bocian, D. F.; Holten, D.; Lindsey, J. S. *J. Mater. Chem.* **2000**, *10*, 283–296. (d) Gupta, I.; Ravikanth, M. *Coord. Chem. Rev.* **2006**, *250*, 468–518.

(9) (a) Gupta, I.; Ravikanth, M. *J. Org. Chem.* **2004**, *69*, 6796–6811. (b) Punidha, S.; Ravikanth, M. *Tetrahedron* **2004**, *60*, 8437–8444. (c) Punidha, S.; Ravikanth, M. *Tetrahedron* **2008**, *64*, 8016–8028. (d) Punidha, S.; Sinha, J.; Kumar, A.; Ravikanth, M. *J. Org. Chem.* **2008**, *73*, 323–328. (e) Berlicka, A.; Pacholska, E.; Latos-Grazynski, L. *J. Porphyrins Phthalocyanines* **2003**, *7*, 8–16. (f) Pandian, R. P.; Chandrashekar, T. K. *Inorg. Chem.* **1994**, *33*, 3311–3324.

Scheme 2. Synthesis of Sn(IV)porphyrin Based Triads **1** and **2**

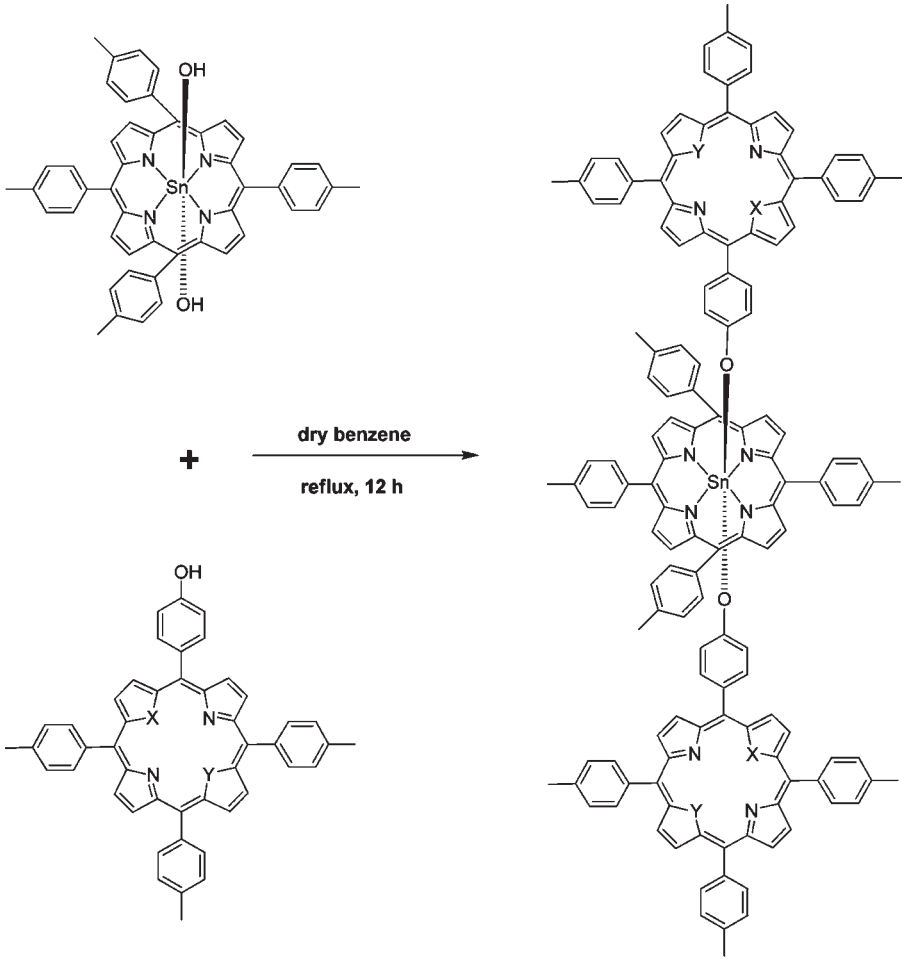

porphyrin with N_4 core and thiaporphyrins with N_3S and N_2S_2 cores. Thiaporphyrins are resulted from the replacement of one or two nitrogens by the thiophene sulfurs and possess very interesting chemical and physical properties which are different from N_4 porphyrins. A perusal of literature reveals that there are no examples on Sn(IV) porphyrin based axial bonding type porphyrin arrays containing thiaporphyrins as axial ligands. Thus an assembly containing a thiaporphyrin with N_2S_2 or N_3S core as axial porphyrin and Sn(IV) derivative of N_4 porphyrin as basal porphyrin offers a unique axial bonding type triads which may possess interesting physicochemical properties. In this paper, we used Sn(IV)TTP$(OH)_2$ as a basal scaffold to synthesize first examples of porphyrin triads **1** and **2** containing heteroporphyrins as axial ligands by adopting the axial bonding approach. We also report the photophysical and electrochemical properties of these two novel axial bonding type porphyrin trimeric arrays.

Results and Discussion

To synthesize the two trimeric arrays **1** and **2**, we need an access to unknown monofunctionalized 21,23-dithiaporphyrin (N_2S_2 core) **3** and 21-monothiaporphyrin **4** having 4-hydroxyphenyl groups at *meso*-position which were synthesized as shown in Scheme 1. The precursor unsymmetrical thiophene diol, 2-[(4-hydroxyphenyl)hydroxymethyl]-5-[(*p*-tolyl)hydroxymethyl]thiophene **5** was synthesized by treating thiophene mono-ol, 2-[(*p*-tolyl)hydroxymethyl]thiophene[9a] with 2 equiv of *n*-BuLi followed by 1.2 equiv of 4-hydroxybenzaldehyde in tetrahydrofuran (THF) at 0 °C. Column chromatographic purification on silica gel afforded the unsymmetrical thiophene diol **5** as yellow semisolid in 32% yield. The diol **5** was confirmed by a molecular ion peak in the ES-MS mass spectrum, clean ^{1}H NMR, and matching elemental analysis. The other precursor 16-thiatripyrrane **6** was synthesized by following a reported procedure.[10] The 21,23-dithiaporphyrin building block, 5-(4-hydroxyphenyl)-10,15,20-tri(*p*-tolyl)-21,23-dithiaporphyrin **3** was synthesized by condensing 1 equiv of unsymmetrical diol **5** with 1 equiv of 16-thiatripyrrin **6** in propionic acid at refluxing temperature.[11] After workup and one filtration column, the thin-layer chromatography (tlc) analysis showed the formation of 21,23-dithiaporphyrin building block **3** as sole product.

(10) Heo, P. Y.; Lee, C. H. *Bull. Korean Chem. Soc.* **1996**, *17*, 515–520.
(11) Adler, A. D.; Longo, F. R.; Finarelli, J. D.; Goldmacher, J.; Assour, J.; Korsakoff, L. *J. Org. Chem.* **1967**, *32*, 476.

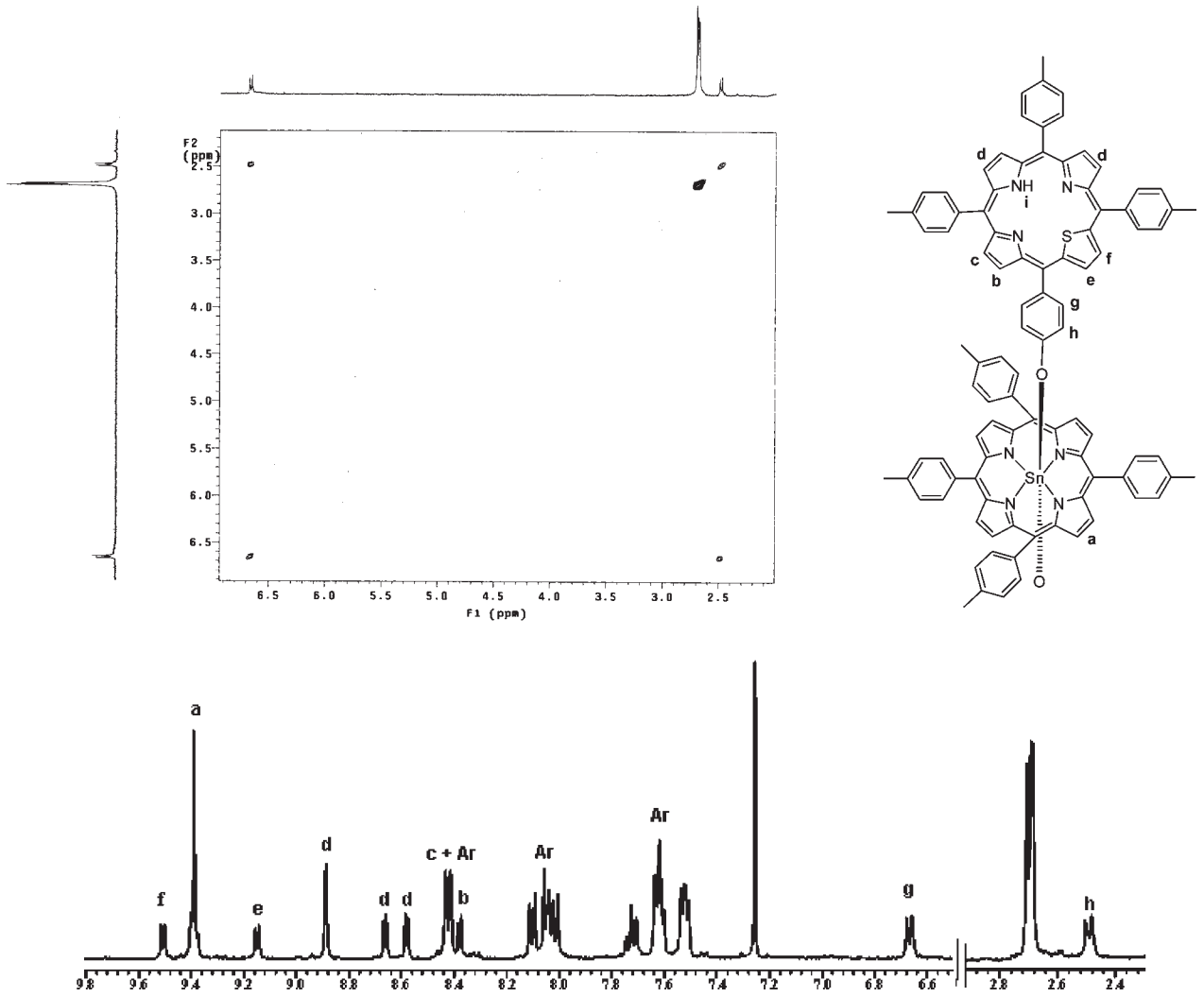

Figure 1. ^{1}H NMR spectra recorded in $CDCl_3$ with various proton assignments for triad **2** and the partial ^{1}H−^{1}H COSY spectrum of **2**.

The crude compound was subjected to silica gel chromatographic purification and afforded pure 21,23-dithiaporphyrin building block **3** as purple solid in 8% yield. The 21-thiaporphyrin building block **4** was synthesized similarly by condensing 1 equiv of unsymmetrical thiophene diol **5** with 2 equiv of *p*-tolualdehyde and 3 equiv of pyrrole in propionic acid under refluxing conditions. The tlc analysis of crude compound showed the formation of two compounds: 5,10,15,20-tetratolylporphyrin (H_2TTP) and the desired 21-thiaporphyrin building block **4**. In general, this condensation should also give a *cis* and *trans* mixture of 21,23-dithiaporphyrin building blocks,[12] but we did not observe the formation of *cis* and *trans* mixture of 21,23-dithiaporphyrins because of the low reactivity of diol **5**. The mixture was separated by column chromatography on silica and afforded pure 21-thiaporphyrin building block **4** in 3% yield. Since the yield of **4** was low, we adopted an alternate method to synthesize **4**. The unsymmetrical diol 2-[(4-methoxyphenyl)hydroxymethyl]-5-[(*p*-tolyl)hydroxymethyl]thiophene **7** was prepared by treating 2-[(*p*-tolyl)hydroxymethyl]thiophene with *p*-anisaldehyde under *n*-BuLi conditions and purified by column chromatography. The diol **7** was then condensed in next step with *p*-tolualdehyde and pyrrole under Lindsey's mild porphyrin forming conditions.[13] The condensation resulted in the formation of a mixture of porphyrins, and the required porphyrin **8** was separated from the mixture by column chromatography to afford pure **8** in 12% yield. In the final step, the porphyrin **8** was treated with 49% HBr-H_2O at reflux to convert the methoxy porphyrin **8** to hydroxy porphyrin **4**. The crude compound was subjected to column chromatographic purification and afforded porphyrin **4** in 60% yield. Although the modified method involves one additional step, the desired N_3S porphyrin building block **4** can be prepared in good yield. The new porphyrins **3**, **4**, and **8** were characterized by ES-MS, ^{1}H and ^{13}C NMR, absorption and elemental analysis techniques.

The triads **1** and **2** were synthesized as shown in Scheme 2. The triad **1** containing 21, 23-dithiaporphyrin subunit as axial ligands was synthesized by refluxing 1 equiv of SnTTP-$(OH)_2$ with 2 equiv of 21,23-dithiaporphyrin building block **3** in benzene at refluxing temperature for 12 h. The benzene was removed on a rotary evaporator, and the crude compound was subjected to basic alumina column chromatography using dichloromethane as eluent. The fast moving band of

(12) Punidha, S.; Agarwal, N.; Ravikanth, M. *Eur. J. Org .Chem.* **2005**, 2500–2517.

(13) Lindsey, J. S.; Schreiman, I. C.; Hsu, H. C.; Kearney, P. C.; Marguerettaz, A. M. *J. Org. Chem.* **1987**, *52*, 827–836.

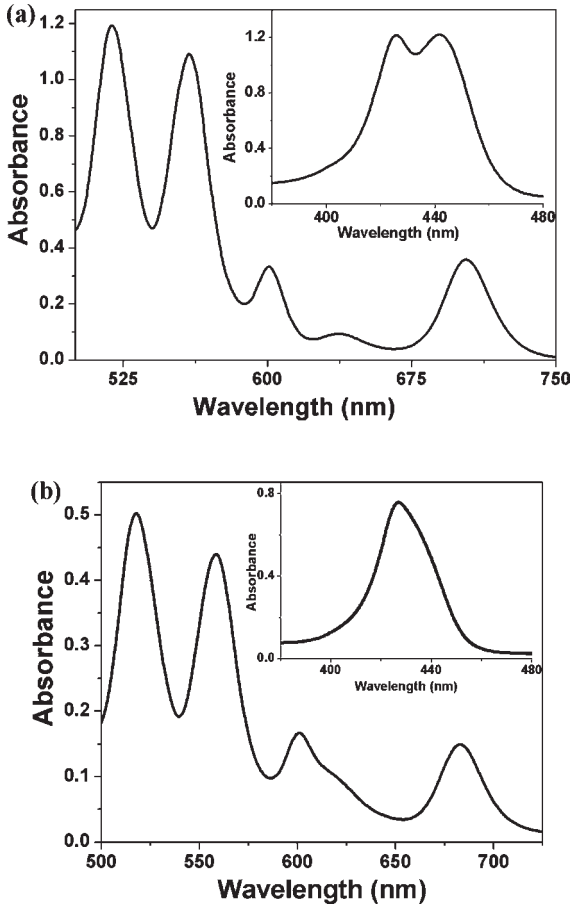

Figure 2. Q-band absorption spectra of triads (a) **1** and (b) **2** recorded in dichloromethane. The inset shows their Soret band absorption spectra.

the desired triad was collected and recrystallized from dichloromethane/*n*-hexanes to afford pure triad **1** in 60% yield. Similarly triad **2** containing N_3S porphyrin as axial ligands was synthesized by reacting $SnTTP(OH)_2$ with 21-thiaporphyrin **4** under the same reaction conditions used for triad **1** followed by column chromatographic purification on basic alumina, and recrystallization afforded triad **2** in 60% yield. The triad formation reactions worked smoothly and required simple column chromatographic purification to afford pure triads in good yields. The triads **1** and **2** were freely soluble in common organic solvents and were characterized by elemental analysis, mass, NMR, absorption, electrochemistry, and fluorescence spectroscopic techniques. The matrix-assisted laser desorption/ionization-time of flight (MALDI-TOF) mass spectra of triads **1** and **2** showed a strong peak corresponding to M-(O porphyrin).[14] The elemental analyses were matched closely with the expected composition of triads confirming the identity of the triads **1** and **2**. The ^1H NMR spectra of triad **2** is presented in Figure 1 along with proton assignments, which are made on the basis of the resonance position and integrated intensity data as well as the proton-to-proton connectivity information revealed in the $^1H-^1H$ COSY spectra to arrive at the structures of these new compounds. It is clear from the NMR data that certain protons of the basal Sn(IV) porphyrin and axial heteroporphyrins in triads **1** and **2** experienced shifts because of the ring current effect of the adjacent porphyrins and appeared at a different region as compared to their corresponding monomeric porphyrins **3** and **4**, respectively. Thus, in triad **2**, all eight β-pyrrole protons of Sn(IV)porphyrin of type *a* resonate at 9.38 ppm which were downfield shifted compared to $SnTTP(OH)_2$ in which the β-pyrrole protons resonate at 9.13 ppm. On the other hand the β-pyrrole protons of axial N_3S porphyrin experienced upfield shifts compared to corresponding monomeric 21-thiaporphyrin. The two β-pyrrole protons of type *b* and two others of type *c* which were facing the central Sn(IV) porphyrin appeared at 8.37 ppm and 8.41 ppm, respectively. The remaining eight β-pyrrole protons of axial porphyrin of type *d* which were away from the central Sn(IV) porphyrin appeared as two doublets at 8.57 ppm, 8.65 ppm and as multiplet at 8.88 ppm. Similarly, the two -thiophene protons of type *e* appeared as a doublet at 9.14 ppm and the other two β-thiophene protons of type *f* appeared as a doublet at 9.50 ppm. All these protons were upfield shifted compared to corresponding monomeric 21-thiaporphyrin **4**. The inner NH proton of axial N_3S porphyrin also experienced slight upfield shift and appeared at -2.78 ppm. However, the most prominent ring current effects were observed for phenoxo groups of the N_3S porphyrin that are bound to the Sn(IV) center. These protons, being affected by both the inherent deshielding effect of the axial N_3S porphyrin and the shielding effect of the basal Sn(IV) porphyrin, resonate at 6.60 ppm as a doublet corresponding to four protons of type *g* and at 2.40 ppm corresponding to four protons of type *h* as detected by the proton connectivity pattern in the $^1H-^1H$ COSY spectrum (Figure 1). Similar observations were made for triad **1** (Supporting Information). In triad **1** also, the maximum upfield shifts were noted for meta (*g* type) and ortho protons (*h* type) of phenoxo groups of the axial porphyrin which appeared at 6.60 and 2.40 ppm, respectively. $^1H-^{13}C$ heteronuclear single-quantum coherence (HSQC) experiments were performed on trimers **1** and **2** to understand the connectivity of various protons and carbon atoms.

The absorption spectra of triads **1** and **2** recorded in dichloromethane are shown in Figure 2, and the data of triads along with their corresponding porphyrin monomers are presented in Table 1. The absorption spectra of triads **1** and **2** showed features of both their corresponding porphyrin monomers and appear to be nearly a superposition of the spectra of the corresponding monomers with slight shifts in their peak maxima. For example, the absorption spectrum of triad **1** showed bands at 426, 442, 519, 559, 601, 637, and 703 nm. In this, the bands at 426, 559, and 601 are mainly due to the Sn(IV) porphyrin subunit, and the bands at 442, 637, and 703 nm are mainly due to the axial 21, 23-dithiaporphyrin subunit. These observations indicate that the porphyrin subunits in triads **1** and **2** interact weakly. The electrochemical studies were carried out on triads **1** and **2** along with their corresponding porphyrin monomers in CH_2Cl_2 using TBAP as supporting electrolyte, and redox potentials were analyzed based on the data of their corresponding monomers. The reduction waves of triads **1** and **2** are presented in Figure 3, and the data of triads **1** and **2** along with their appropriate porphyrin monomers are presented in Table 1. Generally, the triads exhibited two oxidations and two or three reductions. The oxidations are irreversible and difficult to assign, but the reductions are reversible, diffusion controlled, and one electron-transfer reactions. Nonetheless, on the basis of the

(14) Kim, H. J.; Jeon, W. S.; Lim, J. H.; Hong, C. S.; Kim, H.-J. *Polyhedron* **2007**, *26*, 2517–2522.

Table 1. UV-vis and Redox Potential Data (V) for Triads **1** and **2** along with Their Corresponding Monomers

	UV−vis data, λ_{max} nm (log ε)		potential (V) V vs SCE						
compound	Soret band	Q-bands	oxidation		reduction			E_{CT} [$SnP^{-}(N_2XY)_2^{+}$]	E_{CT} [$SnP^{+}(N_2XY)_2^{-}$]
$SnTTP(OH)_2$	429 (6.15)	563 (4.30) 603 (4.24)	1.39		−0.96	−1.36			
3	437 (5.43)	516 (4.42) 550 (4.01) 635(3.19) 699 (3.78)	1.18		−0.94	−1.23			
1	426 (5.89) 442 (5.89)	519 (4.88) 559 (4.84) 601 (4.33) 637 (3.78) 703 (4.36)	1.00	1.53	−0.97	−1.29	−1.38	1.97	2.50
4	430 (5.27)	515 (4.17) 551 (3.78) 618 (3.34) 679 (3.58)	1.11	1.51	−1.03	−1.35			
2	427 (5.65) 437 (5.54)	518 (4.48) 558(4.42) 601 (4.0) 683 (3.95)	0.93	1.28	−1.11	−1.40		2.03	2.39

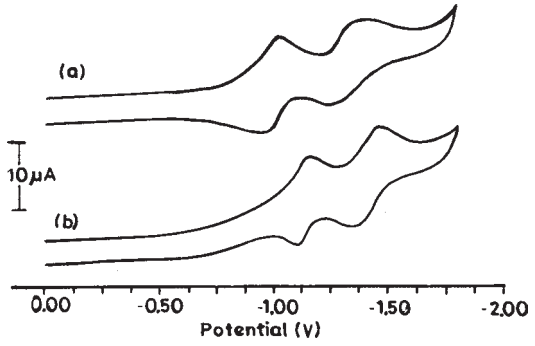

Figure 3. Reduction waves for triads (a) **1** and (b) **2** in dichloromethane containing 0.1 M TBAP as supporting electrolyte recorded at 50 mV/s scan speed.

redox data of the individual monomers, we attempted to assign the peaks to the basal Sn(IV) porphyrin and axial heteroporphyrin separately. Analysis of the redox data in Table 1 revealed that the redox potentials of triads **1** and **2** were in the same range as those of their corresponding monomers supporting a weak interaction among porphyrin subunits in triads **1** and **2**.

The steady state fluorescence properties of triads **1** and **2** were studied in dichloromethane by using excitation wavelengths 515 and 560 nm. From the absorption data, it is clear that these triads can be selectively excited at Sn(IV) porphyrin or the heteroporphyrin absorption maximum. The Sn(IV) porphyrin absorbs more strongly at 560 nm whereas the heteroporphyrin subunit absorbs strongly at 515 nm. The fluorescence spectra of triad **1** at 515 and 560 nm and 2:1 mixture of **3** and $SnTTP(OH)_2$ are shown in Figure 4a whereas the triad **2** at 515 and 560 nm along with 2:1 mixture of **4** and $SnTTP(OH)_2$ at 560 nm are shown in Figure 4b. The photophysical data of triads **1** and **2** along with the corresponding monomeric porphyrins are presented in Table 2. The triads **1** and **2** showed mainly three emission bands; two corresponding to Sn(IV) porphyrin subunit (600, 650 nm) and the third one at 680 nm in triad **2** and 704 nm in triad **1** are mainly due to axial heteroporphyrin subunits (Figure 4). For the triads **1** and **2** on excitation at 515 nm where axial porphyrin subunit was the dominant absorber, the fluorescence was exclusively observed from the axial heteroporphyrin subunit. The quantum yields measured at 515 nm for axial porphyrin subunits in triads **1** and **2** (Table 2) were found to be lower than that of their corresponding porphyrin monomers **3** and **4**, respectively, indicating the quenching of the fluorescence of axial heteroporphyrin because of its

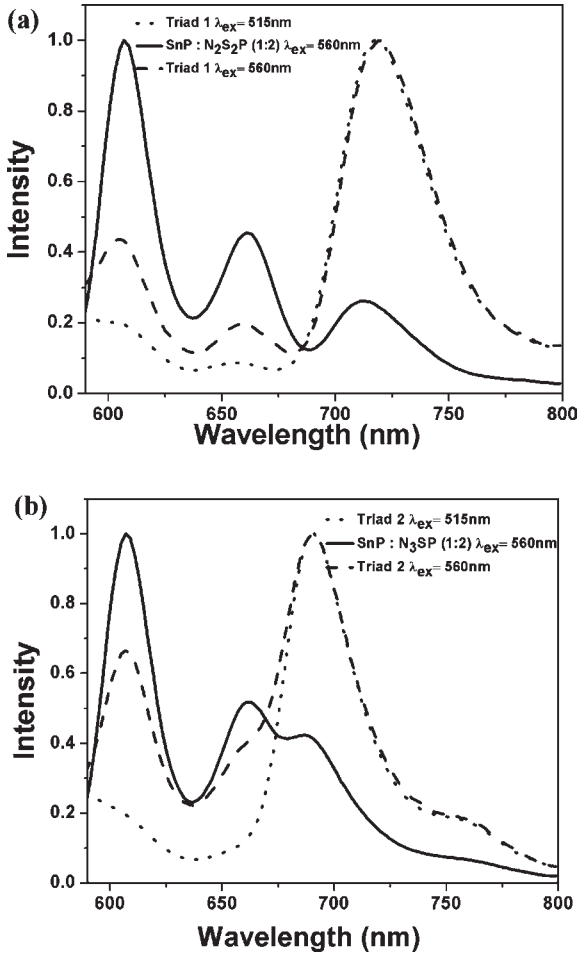

Figure 4. Comparison of normalized emission spectra of triads (a) **1** and (b) **2** along with the 1:2 mixture of their monomers at λ_{ex} = 560 and 515 nm recorded in dichloromethane.

Table 2. Fluorescence Data for Triads **1** and **2** along with Their Corresponding Monomers Recorded in Dichloromethane

compound	λ_{ex} nm	Φ_{N2XYP} (%Q)[a]	Φ_{SnP} (%Q)[a]
SnTTP(OH)$_2$	560		0.025
3	515	0.0076	
1	515	0.0025 (67)	
	560	0.0012 (84)	0.0010 (84)
4	515	0.0168	
2	515	0.0067 (58)	
	560	0.0036 (77)	0.0052 (79)

[a] (%Q) denotes percentage of quenching of fluorescence quantum yield.

coordination to heavy Sn(IV) porphyrin subunit in the triads. However, when triads **1** and **2** were excited at 560 nm where the Sn(IV) porphyrin subunit absorbs 3−4 times more strongly than the axial heteroporphyrin subunits, the fluorescence of the Sn(IV) porphyrin subunit was quenched by 78−84% as compared to the SnTTP(OH)$_2$, and major emission was noted from the heteroporphyrin subunit. However, when a 2:1 mixture of the corresponding monomers of triads **1** and **2** were excited at 560 nm, the major emission was noted from the Sn(IV) porphyrin, and some amount of emission was observed from heteroporphyrin subunit. The excitation spectra of triads **1** and **2** recorded at 720 and 700 nm, respectively, matched closely with the corresponding absorption spectra of triads **1** and **2**. All these observations suggest that in triads **1** and **2**, on excitation at 560 nm, there is a possibility of energy transfer at the singlet state from the basal Sn(IV) porphyrin subunit to the axial N_2S_2 porphyrin subunits in triad **1** and N_3S porphyrin subunits in triad **2**. Furthermore, the energy transfer efficiency can be estimated by the two factors, the donor factor and the acceptor factor.[15] Comparing the emission spectra of triads **1** and **2** with that of the unlinked equimolar mixture (2:1) of their components, the decreased value (ΔI_1) of the integrated fluorescence intensities from the corrected fluorescence spectra of the SnTTP moiety (donor) was obtained, and the percentage of the transferred energy from the donor is $P_d = \Delta I_1/I_1$, where I_1 is the integrated fluorescence intensity of the unconjugated donor [Sn(IV)porphyrin]. For the acceptor, the percentage of accepted energy is $P_a = \Delta I_2/\Delta I_1\phi_F$, where ΔI_2 is the increased value of the integrated fluorescence intensities from the acceptor part in the trimer compared with the unconjugated acceptor (i.e., N_3S and N_2S_2 porphyrins) and ϕ_F is the fluorescence quantum yield of the acceptor. Combining these two factors, the efficiency (E) of energy transfer from the donor to the acceptor can be given by eq 1:

$$E = P_d P_a = \Delta I_2/I_1\phi_F \quad (1)$$

Thus, the efficiencies of energy transfer in **1** and **2** are 68 and 70%, respectively, as calculated from the data in Figure 4 and using the above equation. Besides energy transfer which is majorly responsible for quenching the fluorescence of the Sn(IV) porphyrin subunit, the photoinduced electron transfer (PET) from the ground state of the axial heteroporphyrin subunit (N_2XYP) to the singlet state of the Sn(IV) porphyrin (SnP) may also be partly responsible for quenching the fluorescence of the donor subunit. This PET reaction leads to a charge transfer state of the type ($N_2XYP^+SnP^-$) and involves the free energy change ΔG(PET) which is calculated using the following equation:

$$\Delta G(\text{PET}) = E^{ox}(N_2XYP) - E^{red}(Sn^{IV}P) - E_{0-0}(Sn^{IV}P) \quad (2)$$

The change in free energy ΔG(PET) was found to be −0.07 eV for **1** and −0.01 eV for **2** (Figure 5). Thus, the quenching of the Sn(IV) porphyrin in triads **1** and **2** can be rationalized in terms of the intramolecular energy transfer from the basal Sn(IV) porphyrin to the axial heteroporphyrin competing with the photoinduced electron transfer from the ground state of the axial heteroporphyrin to the basal Sn(IV) porphyrin. Systematic time-resolved absorption and fluorescence studies are required to probe the excited state dynamics of these novel axial bonding type porphyrin triads.

Conclusions

In this paper, for the first time, we have demonstrated the application of the dihydroxoSn(IV) porphyrin as a scaffold in the construction of axial bonding type of arrays involving heteroporphyrins as axial ligands. The absorption and electrochemical studies support weak ground state interaction among the porphyrin subunits within the triads. The fluorescence studies indicate that the basal Sn(IV)porphyrin can act as an energy donor and transfer its energy to the heteroporphyrin subunit. Thus, we conclude that the energy transfer from the Sn(IV) porphyrin subunit to the axial heteroporphyrin subunit is the major cause for quenching the fluorescence of the Sn(IV) porphyrin subunit although the photoinduced electron transfer within the porphyrin subunits in the triads cannot be ruled out completely. We hope the availability of more such axial bonding type arrays containing different types of macrocycles as axial ligands would help in building materials for future applications.

Experimental Section

All general chemicals and solvents were procured from SD Fine Chemicals, India. Column chromatography was performed using silica gel and basic alumina obtained from Sisco Research Laboratories, India. Tetrabutylammonium perchlorate was purchased from Fluka and used without further purifications.

^{1}H NMR spectra were recorded with Varian 400 MHz instrument using tetramethylsilane as an internal standard. ^{13}C NMR spectra were recorded on a Varian spectrometer operating at 100.6 MHz. ^{1}H−^{13}C HSQC experiments were performed on a Bruker AVIII 400 MHz instrument using a BBFO probe. All NMR measurements were carried out at room temperature in deuterochloroform. Absorption and steady state fluorescence spectra were obtained with Perkin−Elmer Lambda-35 and Lambda-55 instruments, respectively. The fluorescence quantum yields (Φ_f) of Sn(IV) porphyrins were estimated from the emission and absorption spectra by a comparative method.[16] ES-MS spectra were recorded with a Q-Tof Micromass spectrometer. MALDI-TOF spectra were obtained from Axima-CFR manufactured by Kratos Analyticals. Cyclic voltammetric (CV) and differential pulse voltammetric (DPV) studies were carried out with a BAS electrochemical system utilizing the three electrode configuration consisting of a glassy carbon (working electrode), platinum wire (auxiliary electrode), and saturated calomel (reference

(15) Durmus, M.; Chen, J. Y.; Zhao, Z. X.; Nyokong, T. *Spectrochimica Acta Part A* **2008**, *70*, 42–49.

(16) Gupta, I.; Ravikanth, M. *Inorg. Chim. Acta* **2007**, *360*, 1731–1742.

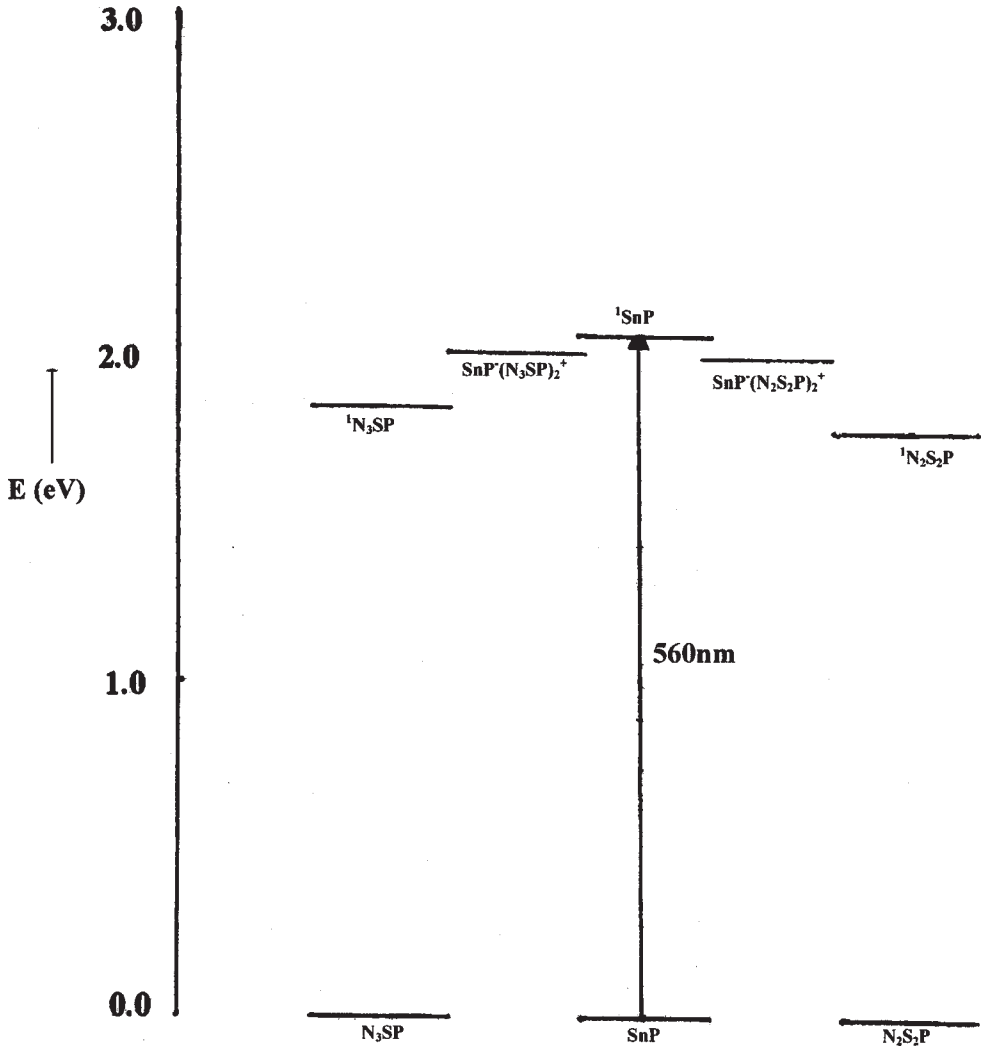

Figure 5. Generalized energy level diagram illustrating singlet and charge transfer states for triads **1** and **2**.

electrode) electrodes in dry dichloromethane using 0.1 M tetrabutylammonium perchlorate as supporting electrolyte.

2-[(4-Hydroxyphenyl)hydroxymethyl]-5-[(*p*-tolyl)hydroxymethyl]-thiophene (5). A sample of 2-[(*p*-tolyl)hydroxymethyl] thiophene (1 g, 4.90 mmol) was charged in a two necked round bottomed flask equipped with nitrogen bubbler and rubber septum. Dry diethyl ether (30 mL) and *N*,*N*,*N*′,*N*′-tetramethylethylenediamine (TMEDA) (1.48 mL, 9.79 mmol) were added to it followed by careful addition of *n*-BuLi (6.12 mL of ca. 15% solution in hexane, 9.79 mmol) at 0 °C. The resultant mixture was allowed to stir at the same temperature for 1 h. Ice cold dry THF solution of 4-hydroxy benzaldehyde (0.72 g, 5.87 mmol) was added to the above mixture and allowed to stir for 6 h at room temperature. The reaction was quenched by adding saturated ammonium chloride solution in water and extracting with dichloromethane. The organic layer was collected and dried over sodium sulfate and evaporated in vacuo. The crude compound was loaded on a silica gel column and eluted with petroleum ether/ethyl acetate (65:35) as a yellowish semi solid. (0.51 g, yield 32%) ^{1}H NMR (400 MHz, $CDCl_3$) δ 2.25 (s, 3H, CH_3), 3.00 (s, 2H, OH), 5.82−5.85 (m, 2H, CHOH), 6.62−6.65 (m, 2H, thiophene), 7.16 (d, J = 8.2 Hz, 2H, Ar), 7.27 (d, J = 7.8 Hz, 2H, Ar), 7.78 (d, J = 7.8 Hz, 2H, Ar), 8.42 (d, J = 8.2 Hz, 2H, Ar) ppm; ^{13}C NMR (100 MHz, $CDCl_3$) δ 22.5, 70.5, 71.5, 120.1, 124.3, 124.5, 128.2, 129.3, 134.6, 136.0, 139.4, 140.2, 143.7, 145.4, 146.1, 156.9 ppm; ES-MS: m/z (%) = 309.3 $(M - 17)^+$ (100); Elemental analysis: Calcd (%) for $C_{19}H_{18}O_3S$: C 69.91, H 5.56, S 9.82; Found: C 69.85, H 5.61, S 9.78.

5-(4-Hydroxyphenyl)-10,15,20-tri(*p*-tolyl)-21,23-dithiaporphyrin (3). The samples of **5** (0.5 g, 1.53 mmol) and 16-thiatripyrrane **6** (0.65 g, 1.53 mmol) in propionic acid (200 mL) were refluxed for 4 h. The propionic acid was removed under vacuum, and the resulted crude compound was washed several times with water and oven-dried. The crude compound was subjected to silica gel column, and the desired porphyrin **3** was eluted using petroleum ether/dichloromethane (15:85) after which the solvent was removed under vacuum to get **3** as a purple solid. (90 mg, Yield 8%) mp > 300 °C; ^{1}H NMR (400 MHz, $CDCl_3$) δ 2.70 (s, 9H, CH_3), 5.13 (s, 1H, OH), 7.22 (d, J = 8.7 Hz, 2H, Ar), 7.61 (d, J = 7.8 Hz, 6H, Ar), 8.09 (d, J = 8.2 Hz, 2H, Ar), 8.12 (d, J = 7.8 Hz, 6H, Ar), 8.68 (s, 4H, β-pyrrole), 9.68 (s, 4H, β-thiophene) ppm; ^{13}C NMR (100 MHz, $CDCl_3$) δ 21.6, 123.6, 124.1, 127.4, 128.1, 130.0, 134.3, 135.2, 136.0, 137.5, 138.3, 142.3, 146.3, 147.5, 149.2, 152.2, 154.3 ppm; ES-MS: m/z (%) = 707.2 $(M + H)^+$ (100); Elemental analysis: Calcd (%) for $C_{47}H_{34}N_2OS_2$: C 79.85, H 4.85, N 3.96, S 9.07; Found: C 79.90, H 4.80, N 3.92, S 9.11.

2-[(4-Methoxyphenyl)hydroxymethyl]-5-[(*p*-tolyl)hydroxymethyl]thiophene (7). The diol **7** was prepared from 2-[(*p*-tolyl)hydroxymethyl]thiophene (1 g, 4.90 mmol) similarly by following the procedure described for diol **5** using 4-methoxybenzaldehyde in place of 4-hydroxybenzaldehyde. (0.8 g, yield 48%) ^{1}H NMR (400 MHz, $CDCl_3$) δ 2.33 (s, 3H, CH_3), 2.47 (bs, 2H, OH), 3.78 (s, 3H, OCH_3), 5.89 (d, J = 5.4 Hz, 2H, CHOH), 6.65−6.67 (m, 2H, thiophene), 6.85 (d, J = 8.8 Hz, 2H, Ar), 7.14 (d, J = 7.6 Hz, 2H, Ar), 7.25−7.33 (m, 4H, Ar) ppm; ^{13}C NMR

(100 MHz, $CDCl_3$) δ 21.3, 55.4, 72.3, 114.0, 124.4, 126.4, 127.8, 129.3, 135.3, 137.9, 140.1, 148.5, 159.4 ppm; ES-MS: m/z (%) = 323.1 $(M\text{-}17)^+$ (100); Elemental analysis: Calcd (%) for $C_{20}H_{20}O_3S$: C 70.56, H 5.92, S 9.42; Found: C 70.60, H 5.88, S 9.45.

5-(4-Methoxyphenyl)-10,15,20-tri(*p*-tolyl)-21-thiaporphyrin (8). Samples of unsymmetrical diol **7** (0.5 g, 1.4 mmol), *p*-tolualdehyde (0.33 mL, 2.8 mmol), and pyrrole (0.29 mL, 4.2 mmol) were dissolved in dichloromethane (300 mL), and the reaction flask was degassed with nitrogen for 10 min with stirring. The condensation was initiated by adding $BF_3.OEt_2$ (0.4 mL of 2.5 M solution) while stirring the reaction mixture at room temperature for 1 h under a nitrogen atmosphere. 2,3-Dichloro-5,6-dicyano-benzoquinone (DDQ) (0.32 g, 1.4 mmol) was then added, and the reaction mixture was stirred in air for an additional 1 h. The solvent was removed under reduced pressure, and the crude compound was purified by silica gel column chromatography using petroleum ether/dichloromethane (60:40) to afford porphyrin **8**. (125 mg, Yield 12%) ^{1}H NMR (400 MHz, $CDCl_3$) δ −2.68 (s, 1H, NH), 2.69 (s, 3H, CH_3), 4.08 (s, 3H, OCH_3), 7.34 (d, J = 8.5 Hz, 2H, Ar), 7.54 (d, J = 7.6 Hz, 4H, Ar), 7.61 (d, J = 7.9 Hz, 2H, Ar), 8.07 (d, J = 7.9 Hz, 4H, Ar), 8.12−8.18 (m, 4H, Ar), 8.60−8.62 (m, 2H, pyrrole), 8.68 (d, J = 4.2 Hz, 2H, pyrrole), 8.93−8.94 (m, 2H, pyrrole), 9.75 (s, 2H, thiophene) ppm; ^{13}C NMR (100 MHz, $CDCl_3$) δ 21.7, 110.2, 113.3, 127.5, 128.5, 133.2, 133.7, 134.4, 135.6, 138.3, 139.2, 139.7, 147.3, 154.6, 159.7 ppm; ES-MS: m/z (%) = 704.4 $(M+H)^+$ (100); Elemental analysis: Calcd (%) for $C_{48}H_{37}N_3OS$: C 81.90, H 5.30, N 5.97, S 4.56; Found: C 81.95, H 5.25, N 5.98, S 4.54.

5-(4-Hydroxyphenyl)-10,15,20-tri(*p*-tolyl)-21-thiaporphyrin (4). Samples of unsymmetrical diol **5** (0.5 g, 1.53 mmol), *p*-tolualdehyde (0.36 mL, 3.06 mmol), and freshly distilled pyrrole (0.32 mL, 4.60 mmol) were refluxed in 200 mL of propionic acid for 4 h. The propionic acid was removed under reduced pressure, and the residue was washed thoroughly with water and oven-dried. The crude compound was subjected to silica gel column chromatography, and the desired porphyrin **4** was collected using dichloromethane as eluent. (35 mg, Yield 3%) mp > 300 °C; ^{1}H NMR (400 MHz, $CDCl_3$) δ −2.69 (s, 1H, NH), 2.73 (s, 9H, CH_3), 7.28 (m, 2H, Ar), 7.55 (d, J = 7.9 Hz, 4H, Ar), 7.62 (d, J = 8.2 Hz, 2H, Ar), 8.00−8.10 (m, 8H, Ar), 8.60−8.61 (m, 2H, β-pyrrole), 8.68−8.69 (m, 2H, β-pyrrole), 8.93 (s, 2H, β-pyrrole), 9.75 (s, 2H, β-thiophene) ppm; ^{13}C NMR (100 MHz, $CDCl_3$) δ 21.7, 114.7, 123.9, 127.5, 128.5, 129.0, 130.0, 131.5, 133.1, 133.8, 134.4, 135.6, 137.7, 138.3, 139.2, 141.9, 147.2, 154.6, 155.7, 157.7 ppm; ES-MS: m/z (%) = 690.5 $(M+H)^+$ (100); Elemental analysis: Calcd (%) for $C_{47}H_{35}N_3OS$: C 81.83, H 5.11, N 6.09, S 4.65; Found: C 81.85, H 5.08, N 6.11, S 4.63.

The compound **4** was also synthesized alternatively by refluxing porphyrin **8** (0.1 g, 14 mmol) in 30 mL of HBr-water (49%) for 4 h. The reaction mixture was extracted with dichloromethane and was washed several times with water and dilute ammonia solution (25% v/v). The organic layer was evaporated under reduced pressure and subjected to silica gel column chromatographic purification using dichloromethane to afford pure **4**. (58 mg, 60%).

General Synthesis of Triads (1) and (2). The triads **1** and **2** were synthesized by refluxing Sn(IV)TTP$(OH)_2$ (12 μmol) and monohydroxyporphyrins **3** and **4** (24 μmol), respectively, in dry benzene (10 mL) for 12 h under a nitrogen atmosphere. The solvent was evaporated under reduced pressure, and the resulted residue was subjected to basic alumina column. The desired product was eluted with dichloromethane and was recrystallized using dichloromethane/*n*-hexane mixture to afford trimers **1** and **2** in 60% yield.

Porphyrin Triad (1). Mp > 300 °C, ^{1}H NMR (400 MHz, $CDCl_3$) δ 2.49 (d, J = 8.5 Hz, 4H, Ar), 2.68−2.70 (m, 30H, CH_3), 6.65 (d, J = 8.5 Hz, 4H, Ar), 7.58−7.73 (m, 23H, phenyl), 8.02−8.11 (m, 13H, phenyl), 8.41−8.45 (m, 8H, [β-pyrrole + phenyl]), 8.65 (s, 4H, β-pyrrole), 9.04 (d, J = 4.9 Hz, 2H, β-thiophene), 9.39 (s, 8H, β-pyrrole Sn), 9.41 (d, J = 4.9 Hz, 2H, β-thiophene), 9.62 (s, 4H, β-thiophene) ppm; MALDI-TOF: m/z (%) = 1493.1 $(M\text{-}C_{47}H_{34}N_2OS_2)^+$ (90); Elemental analysis: Calcd (%) for $C_{142}H_{102}N_8O_2S_4Sn$: C 77.71, H 4.96, N 4.97, S 5.68; Found: C 77.81, H 4.93, N 5.70, S 5.65.

Porphyrin Triad (2). Mp > 300 °C, ^{1}H NMR (400 MHz, $CDCl_3$) δ −2.78 (s, 2H, NH), 2.49 (d, J = 8.5 Hz, 4H, Ar), 2.68−2.70 (m, 30H, CH_3), 6.65 (d, J = 8.5 Hz, 4H, Ar), 7.50−7.74 (m, 22H, phenyl), 8.0−8.09 (m, 10H, phenyl), 8.10 (d, J = 7.9 Hz, 4H, phenyl), 8.37 (d, J = 4.6 Hz, 2H, β-pyrrole), 8.41−8.42 (m, 6H, [β-pyrrole + phenyl]), 8.57 (d, J = 4.6 Hz, 2H, β-pyrrole), 8.65 (d, J = 4.5 Hz, 2H, β-pyrrole), 8.88−8.89 (m, 4H, β-pyrrole), 9.14 (d, J = 5.2 Hz, 2H, β-thiophene), 9.37−9.39 (m, 8H, β-pyrrole Sn), 9.50 (d, J = 5.2 Hz, 2H, β-thiophene) ppm; MALDI-TOF: m/z (%) = 1476.7 $(M\text{-}C_{47}H_{35}N_3OS)^+$ (25); Elemental analysis: Calcd (%) for $C_{142}H_{104}N_{10}O_2S_2Sn$: C 78.91, H 5.13, N 6.30, S 2.89; Found: C 78.93, H 5.15, N 6.27, S 2.88.

Acknowledgment. M.R. thanks Council of Scientific and Industrial Research (CSIR) and Department of Science and Technology (DST) for financial support, and V.S. thanks CSIR for a fellowship.

Supporting Information Available: Mass and NMR spectra of selected compounds. This material is available free of charge via the Internet at http://pubs.acs.org.